

Response of fiber reinforced plastic chimneys to wind loads

A.S. Awad[†]

Mccavour Eng. Ltd. Mississauga, Ontario, Canada

A.A. El Damatty[‡] and B.J. Vickery^{‡‡}

*Department of Civil and Environmental Engineering, The University of Western Ontario,
London, Ontario, N6A 5B9 Canada*

Abstract. Due to their high corrosion and chemical resistance, fiber reinforced plastics (FRP) are becoming widely used as the main structural material for industrial chimneys. However, no national code currently exists for the design of such type of chimneys. The purpose of this study is to investigate analytically the response of FRP chimneys to wind loads. The classical lamination theory is used to substitute the angle-ply laminate of a FRP chimney with an equivalent orthotropic material that provides the same stiffness. Dynamic wind loads are applied to the equivalent chimney to evaluate its response to both along and across wind loads. A parametric study is then conducted to identify the material and geometric parameters affecting the response of FRP chimneys to wind loads. Unlike the across-wind response, the along-wind tip deflection is found to be highly dependent on the angle of orientation of the fibers. In general, the analysis shows that FRP chimneys are very vulnerable to across-wind oscillations resulting from the vortex shedding phenomenon.

Key words: fiber reinforced plastics; chimneys; laminated; wind loads; vortex shedding; dynamic.

1. Introduction

The development of FRP materials which have high corrosion and acid resistance and also have stable behavior under relatively high temperature, has recently encouraged the use of these composite materials in the construction of industrial chimneys. In 1984, Plenick *et al.* (1984) reported a 52 m height free-standing fiber glass stack that was manufactured for a sugar processing plant in Moses Lake, Washington, U.S.A. During the past decade, a large number of FRP chimneys have been built in North America and in various places around the world. FRP chimneys are commonly applied in the pulp & paper and the chemical industries where highly corrosive gases are produced. FRP flue gases have been also built in power generation stations.

While, the designer of steel or concrete chimneys can rely on a number of detailed codes of design, (e.g., CICIND 1988, ACI 1995), no design provisions are currently available for FRP chimneys.

[†] Structural Engineer

[‡] Assistant Professor, e-mail; damatty@julian.uwo.ca

^{‡‡} Professor

Meanwhile, studies conducted on FRP chimneys are very rare in the literature.

The design of industrial chimneys is usually governed by the stresses and displacements induced by the wind loads. Meanwhile, a proper design should also account for various phenomena associated with wind loads acting on slender structures such as vortex shedding and ovaling.

One of the problems that interests researchers as well as designers of industrial chimneys is the understanding of the complete behavior of the vortices in the downstream of cylinders created by the oncoming flow. It has been more than a century since Strouhal stated the relationship between the frequency of the vortices, the wind speed and the diameter of the cylinder. Since that, many efforts were done to estimate the magnitude of the fluctuating forces acting on cylinders associated with the turbulent wind in the wake of the structure (Scurton 1963, Van Koten 1969, Davenport 1993, Vickery 1997).

In the present study, an analytical investigation for the response of FRP chimneys to wind loads is conducted. A simple and efficient computer code, to be used in achieving this task, is developed and described in this paper. The developed computer code can be used to perform static and dynamic analysis of tapered cantilever like laminated structures (e.g., free standing FRP chimneys) subjected to wind loads. The developed computer code is based on the following :

- 1) Classical lamination theory to obtain apparent elastic properties of the laminate based on the mechanical properties of each lamina in its local material axes and also on the stacking sequence of the layers.
- 2) The Stodola method to evaluate the natural frequencies and the corresponding mode shapes of a FRP tapered chimney.
- 3) The wind loads acting on the chimney (along-wind and vortex shedding) treated as an equivalent static loads according to the CICIND code for steel chimneys (1988), or as a combination of static and dynamic loads based on a procedure developed by Davenport (1993) and a model proposed by Basu and Vickery (1983).

The computer code is verified using a detailed finite element analysis. This is followed by a parametric study conducted using the developed code to investigate the effects of the angle of orientation of the plies, the mass density of the composite, the damping, and the tapering ratio on the along and across-wind responses of FRP chimneys.

2. Analysis procedure

2.1. Classical lamination theory

FRP stacks are usually constructed from a large number of angle-ply layers (a typical thickness of a lamina varies between 0.8-1.0 mm). For angle-ply configuration, the fibers of a certain layer is oriented with an angle θ with a reference direction and the fibers of the adjacent layers are oriented by an angle $-\theta$ with the same direction. The use of angle-ply laminate in the construction for FRP chimneys is favorable than any other stacking sequence. This configuration minimizes the coupling between extension and bending stresses as well as between shear stresses and normal strains. Beside the ease of construction, angle-ply configuration provides laminate with high in-plane shear stiffness. The constituents of the layers used for FRP stacks are usually Vinyl Ester resin and E-glass fibers. A 70% fibers contents (based on weight) is commonly used in the construction of FRP stacks (as well as pipes).

A vertical projection and a horizontal cross section of a tapered FRP chimney, together with a

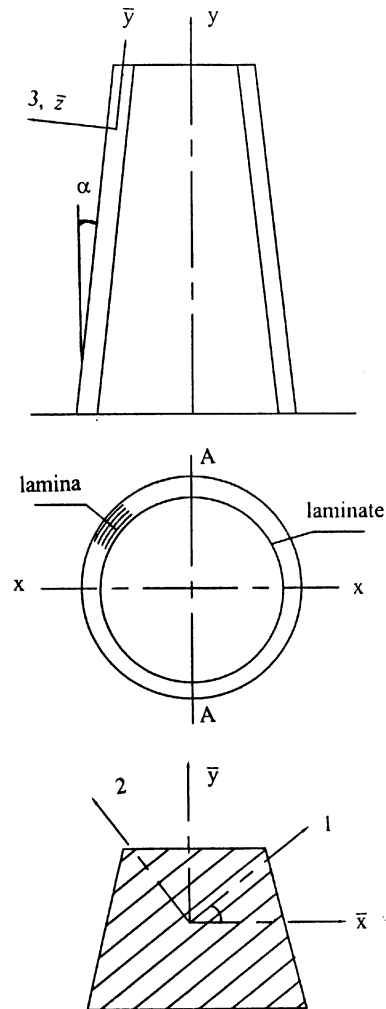


Fig. 1 Vertical and horizontal cross sections of FRP chimney and vertical projection of the laminate.

vertical projection of a typical lamina are shown in Fig. 1. As shown in the figure, at a certain point in a lamina, a set of material axes system (1, 2 and 3) and another set of local axes system (\bar{x} , \bar{y} and \bar{z}) are defined. Axes 1, 2, \bar{x} and \bar{y} are all located in a plane tangent to the surface. Axis 1 is directed along the fibers, axis 2 is in a direction perpendicular to the fibers, the \bar{x} -axis is parallel to a horizontal plane while the \bar{y} axis is a meridional axis making an angle α with the vertical direction (α is the tapering angle of the chimney). Axes 3 and \bar{z} are both perpendicular to a plane tangent to the surface.

The classical lamination theory (CLT) can be used to predict the elastic properties of an equivalent orthotropic material having the same stiffness as the laminate. The classical lamination theory, which is presented in details by Jones (1984), is based on the assumption that transverse shear stresses τ_{13} and τ_{23} as well as the normal stresses σ_{33} can be neglected.

Different values for extension and bending elastic properties of the equivalent orthotropic material are predicted by the CLT. The equivalent extension properties of a laminate are presented by the

EUROCOMP (1997) and are given as :

$$\begin{aligned} E_{\bar{x}} &= 1/(h.a_{11}) & E_{\bar{y}} &= 1/(h.a_{22}) \\ G_{\bar{xy}} &= 1/(h.a_{66}) & \nu_{\bar{xy}} &= -a_{12}/a_{11} & \nu_{\bar{yx}} &= -a_{12}/a_{22} \end{aligned} \quad (1)$$

Where $E_{\bar{x}}$ and $E_{\bar{y}}$ are the extension elastic moduli in the \bar{x} and \bar{y} directions, respectively; $G_{\bar{xy}}$, $\nu_{\bar{xy}}$ and $\nu_{\bar{yx}}$ are the shear modulus and the Poisson's ratios, respectively; h is the total thickness of the laminate; a_{ij} are the components of the inverse of the extension stiffness matrix $[A]$ of the laminate which is given as :

$$A_{ij} = \sum_{k=1}^N (\bar{Q}_{ij})_k (z_k - z_{k-1}) \quad (2)$$

where z_k and z_{k-1} are the distance from the middle surface of the laminate to the top and bottom surface of the k th lamina, $(\bar{Q}_{ij})_k$ is the reduced transformed stiffness matrix of the k th lamina and is defined in EUROCOMP (1997), and N is the total number of the layers.

2.2. Beam bending behavior of chimneys

The behavior of a free standing chimney subjected to wind loads can be simulated as beam bending about axis A-A (shown in Fig. 1). Considering a horizontal cross section of the chimney, such a global bending behavior will cause mainly extension (or shortening) strains which vary from point to another on the circumference of the section (the through-thickness local bending strains can be neglected as the thickness of the chimney is much smaller than its radius). As such, the main parameter which governs the strains induced in the equivalent beam model is E_y (equivalent extension modulus of elasticity along the y axis shown in Fig. 1) which can be obtained by evaluating $E_{\bar{y}}$ from Eq. (1) and then applying the following transformation:

$$E_y = E_{\bar{y}} \cos^2 \alpha \quad (3)$$

where α is the angle between axes \bar{y} and y . Note that this beam model can be used to evaluate the displacements and the strains of the chimney. Stresses should be evaluated from the calculated strains and the true moduli of each lamina.

The natural frequencies and mode shapes of free standing tapered chimneys, having a modulus E_y calculated using Eqs. (2) and (3), are then evaluated using the Stodola method (Berg 1989).

2.3. Wind loads

The wind loads acting on a typical chimney have two basic components; the mean component which is static and the fluctuating component which has a dynamic nature. The fluctuating part is divided to an irregular and slowly varying component, known as the background component, and an oscillatory component having a definite frequency and known as the resonant component. The dynamic wind response of a chimney is controlled by the following aerodynamic parameters the turbulent fluctuations in the oncoming flow which cause the along and across-wind responses, the vortices shedding in the wake of the structure which create an across-wind responses, and aerodynamic damping forces due to the motion of the structure. Herein, the method used for calculating the along-wind response of FRP chimney is based on an approach developed by Davenport

(1993). The approach uses influence lines for calculating the response and is well suited for evaluating the drag load response of chimneys. The procedure is described in details by Davenport (1993).

The response of structures to the vortices which shed behind the structures in a smooth or turbulent flow is not completely understood yet. This difficulty of predicting the vortex response is due to the limited full scale data and the difficulties in achieving Reynolds Number associated with large chimneys in wind tunnel testing (Vickery 1997). The frequency f_e of the eddies that shed behind a cylinder when a flow passes cylinder is given by:

$$f_e = S \frac{\bar{u}}{d} \quad (4)$$

where S is Strouhal number, \bar{u} and d are the mean wind speed and the diameter of the cylinder, respectively. The wind speed which produces eddies having a frequency matching any of the structure natural frequencies is called a critical wind speed. At this case, a resonant response associated with a rapid change of the aerodynamic damping from positive to negative occurs (Vickery and Steckley 1993). The negative aerodynamic damping reduces the total effective damping of the system and consequently magnifies the lateral oscillations of the structure.

In the current study, the across-wind response is evaluated using a model proposed by Basu and Vickery (1983). This model has been correlated with observed full-scale behavior. The first part of the model simulates the lift forces acting on a stationary body using a Gaussian distribution for the lift force spectrum. This spectrum is defined by three parameters: the r.m.s lift coefficient \tilde{C}_{LV} , the bandwidth parameter B , and the Strouhal number S . Based on full-scale measurements, Basu and Vickery (1983) concluded that the r.m.s of the lift coefficient \tilde{C}_{LV} has a strong dependency on the scale and intensity of turbulence. In addition, they have concluded that the bandwidth parameter B depends only on the intensity of turbulence. Also based on full-scale data, Vickery and Basu (1983) suggested the following expression for the bandwidth parameter B :

$$B = 0.1 + 2i \quad (5)$$

where i is the local intensity of turbulence.

The Strouhal number S depends on the surface roughness, Reynolds number, turbulence and aspect ratio of the structure. Vickery (1997) has provided relations for evaluating the r.m.s lift coefficient \tilde{C}_{LV} , the Strouhal number S and the lift force spectrum. These relations are employed in the current study.

The second part of the model for across-wind response (Basu and Vickery 1983) simulates the aero-elastic effect. According to this model, the aerodynamic damping force, w_D , per unit length is given as :

$$w_D = -4\pi K_a \rho d^2 f_o \tilde{y} \quad (6)$$

$$K_a = K_{ao} \left(1 - \left(\frac{\tilde{y}}{0.4d} \right)^2 \right) \quad (7)$$

where ρ is the air density, f_o is the natural frequency, K_{ao} is mass-damping parameter at small amplitudes, \tilde{y} is the r.m.s. displacement of cylinder and d is the diameter, respectively.

As seen from Eqs. (6) and (7), the aerodynamic damping forces depend on the amplitude of vibration in a non-linear manner. The nonlinear term is significant at higher level of lateral oscillations which would correspond to an unstable state for the chimney. As the current study is

only concerned with the stable behavior of FRP chimneys, i.e., at acceptable level of lateral oscillations, the nonlinear linear term has been neglected. In view of Eqs. (6) and (7), Vickery (1997) has provided the following expression for the aerodynamic damping ratio β_{aero} (that neglects the non-linear effect) :

$$\beta_{aero} = -\rho \frac{\int_0^H K_a(z) d^2(z) \phi_i^2(z) dz}{\int_0^H m(z) \phi_i^2(z) dz} \quad (8)$$

$$K_a(z) = \frac{k}{10} - K_{ao}^* \frac{k^2}{1+6i} \exp\left\{-\left(\frac{6(k-1)^2}{1+6i}\right)\right\} \quad (9)$$

where H is the height of the structure; ϕ_i is the i th mode shape; m is the mass per unit length; $k = \bar{u}(z)/\bar{u}_c$; \bar{u} is the local mean wind speed; \bar{u}_c is the local critical wind speed and is given by $\bar{u}_c = \{1/S\}f_i d$; f_i is the natural frequency of the i th mode; and k_{ao}^* is a reference value for smooth flow and is approximately equal to 1.2, respectively.

The procedure for evaluating E_y using the classical lamination theory, the Stodola method for determining the natural frequencies and mode shapes, the procedure described by Davenport (1993) to evaluate the along-wind responses, and the Basu and Vickery (1983) model for the vortex shedding response have been all incorporated into a computer code that can predict the response of FRP chimneys subjected to wind loads.

3. Comparison between the developed code and the finite element analysis

A detailed finite element model, based on a consistent laminated shell element (Koziey 1993, Koziey and Mirza 1997) is used to check the adequacy of using the CLT to replace the laminate's layers with an equivalent orthotropic material. It should be mentioned that the consistent laminated shell element model involves a simulation for the exact layer's configuration of the laminate.

Three different chimneys are modeled and analyzed under static load conditions using both the laminated shell element and the developed computer code. The chimney's laminates consist of angle-ply laminae all having 50% E-glass as reinforcement (based on weight) and Der 411-45 as resin. The layers have the following mechanical properties defined in the directions of the material axes (1-2): $E_1 = 23.46$ GPa, $E_2 = 6.95$ GPa, $G_{12} = G_{13} = 2.2$ GPa, $G_{23} = 2.65$ GPa, $\nu_{12} = \nu_{13} = \nu_{23} = 0.32$. The dimensions of the chimneys and the stacking sequence of the layers are shown in Table 1. The three chimneys are subjected to wind speed equal to 30 m/sec at elevation 10 m above the

Table 1 The dimensions, the lay-up and the tip deflections of FRP chimneys

Height L (m)	Diameter D (m)	Thickness t (mm)	lay-up	Deflection(m)		Meridional Stresses (MPa)	
				Present	F.E.	Present σ_y	F.E. σ_y
30	1.5	30	0° \ 90° \ 0°	0.41	0.401	32.55	31.1
40	2.0	45	55° \ 55° \ 55°	0.63	0.616	20.5	22.6
50	2.5	70	45° \ -45° \ 45°	1.04	0.950	23.2	18.5

ground and are assumed to have 1.0% damping ratio. The equivalent static load based on the CICIND (1988) is applied to both the finite element model and the developed computer code. The deflections at the top of the chimneys as well as the meridional stresses resulting from both analyses are presented in Table 1. Comparison between the results of the analyses indicates an excellent agreement and shows that the simple approach adopted in the paper is accurately predicting the response of laminated FRP chimneys.

4. Parametric study

The geometry of a FRP chimney, the properties of its laminate and the wind characteristics have a direct influence on the structural response of the chimney. The main material and geometric parameters are: the elastic properties of the basic materials (fibers, matrix), fibers content ratio, fibers orientation, laminate stacking sequence (symmetric, anti-symmetric, unsymmetric), mass density of the composite, material damping, tapering ratio, and the aspect ratio (height/diameter) of the chimney. The intensity of the turbulence, Strouhal number, Reynolds number, r.m.s of lift coefficient and the mean wind speed are the main wind parameters that affect the along and across-wind responses.

Using the computer code developed in this study, a parametric study is done for investigating the effect of some of the above mentioned parameters on the along and across-wind responses of FRP chimneys.

4.1. Fibers orientation

The fibers orientation of the individual lamina plays a significant role in defining the apparent elastic properties of the laminate. In order to study the effect of the fibers orientation, three cylindrical chimneys are considered. The chimneys have 40, 60 and 80 m height, 2.5, 3.75 and 5.0 m diameter, and 30, 37 and 50 mm wall thickness, respectively. The fibers type is E-glass-roving (70% of the weight of the composite) used as reinforcement for Der 411-45 resin. The elastic properties of the orthotropic layers defined in the material axes 1-2 are shown in Table 2. The chimneys have an angle-ply laminate ($\pm\theta$) with 1.0 mm thickness for each lamina.

Fig. 2 shows typical relation between the apparent longitudinal flexural modulus E_y that resulted from the developed computer code (normalized with respect to the lateral modulus E_2 of the basic lamina) and the angle-ply $\pm\theta$ (for the chimney having a height equal to 40 m). It is clear from the figure that the longitudinal modulus is strongly dependent on the laminae orientation. The maximum

Table 2 The mechanical properties of E-glass/Vinyl Ester layer

Modulus	GPa
Longitudinal	$E_1 = 36.85$
Transverse	$E_2 = 11.16$
In-plane shear	$G_{12} = 3.36$
Transverse shear	$G_{13} = 3.36, G_{23} = 4.32$
Poisson's ratios $\nu_{12} = 0.3, \nu_{13} = 0.3, \nu_{23} = 0.29$	
Mass density = 1867 kg/m^3	
Fibers content (by weight) = 70%	

modulus is achieved at $\theta=90^\circ$, i.e., when all fibers are oriented parallel to the y direction. The minimum value of the apparent longitudinal modulus occurs at the vicinity of $\theta=30^\circ$. It should be mentioned that due to the contribution of the shear modulus, the minimum longitudinal apparent modulus E_y can be larger or smaller than the lateral lamina modulus E_2 and also the maximum can be larger or smaller than the longitudinal lamina modulus E_1 . Fig. 2 suggests that in order to benefit from the presence of fibers in enhancing the longitudinal stiffness of the chimney, fibers have to be oriented by an angle $\theta \geq 55^\circ$. In Fig. 3, the fundamental natural frequency of the same chimney is plotted versus the angle of orientation θ . As expected, the natural frequency has the same trend as the variation of the apparent longitudinal modulus. It should be mentioned that from the practical

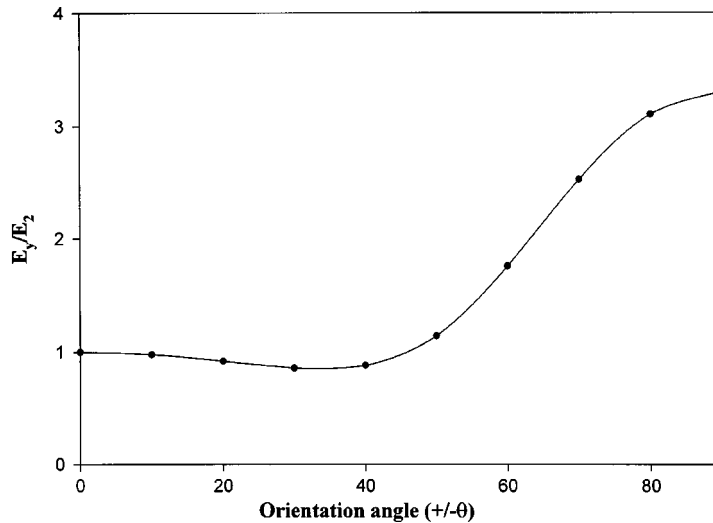


Fig. 2 Variation of the longitudinal extension modulus with fibers orientation

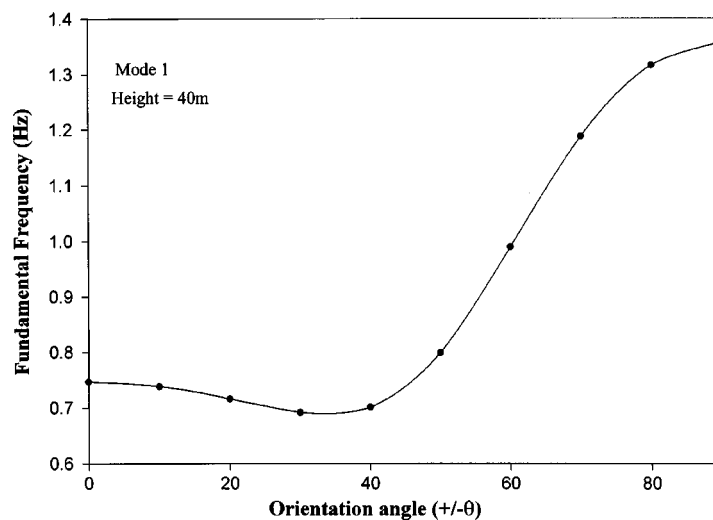


Fig. 3 Variation of the fundamental natural frequency with fibers orientaton

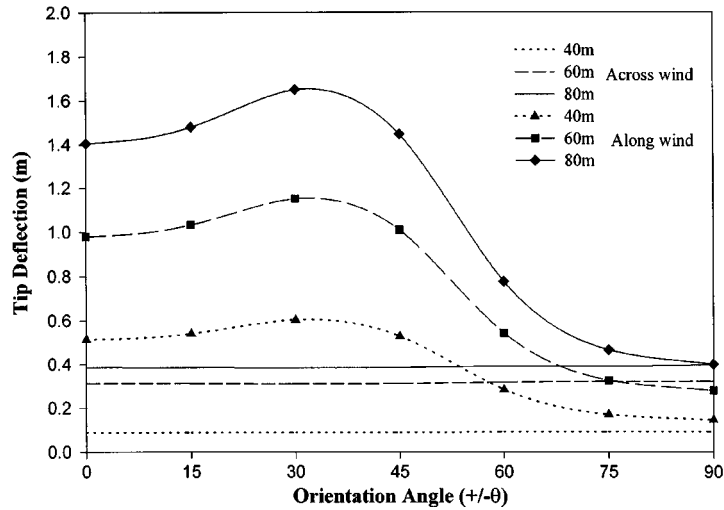


Fig. 4 Along and across-wind tip deflection versus fibers orientation

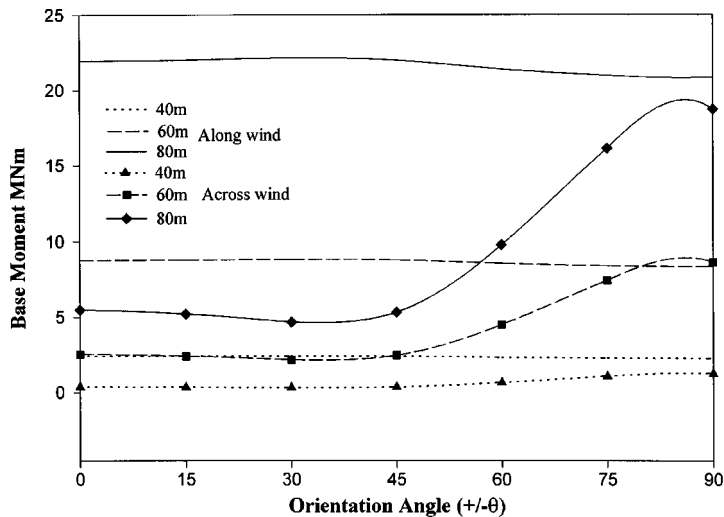


Fig. 5 Along and across-wind base bending moment versus fibers orientation

point of view, the most used angle of orientation varies between $\pm 35^\circ$ and $\pm 55^\circ$.

The along and across-wind tip deflection for the three chimneys are evaluated using a wind speed $U_{10} = 30.0$ m/s (at 10 m above the ground), an intensity of turbulence $i = 0.14$ and a damping ratio $\zeta_s = 0.80\%$. The variation of the maximum tip deflection and the peak base overturning moment, for both the along and across wind directions, with the angle of orientation θ are plotted in Figs. 4 and 5, respectively. It should be noted that in these figures the along and across wind responses are evaluated at the design wind speed ($U_{10} = 30$ m) and at the vicinity of the critical wind speed (usually at slightly higher wind speed than the critical one), respectively. From these figures, the following observations can be drawn:

- 1) For the across wind direction, the variation of the angle of orientation does not affect the peak

tip deflection. On the other hand, a significant change in the values of the across wind peak overturning moment is associated with the variation of the angle.

- 2) For the along wind direction, the variation of the angle of orientation does not affect the peak overturning moment and meanwhile leads to a significant variation of the peak tip deflection.

It is clear that the variation of the angle of orientation has a reverse effect on the peak tip deflection and the peak base overturning moment. This behavior can be interpreted by the following:

A change in the angle of orientation leads to a variation in the stiffness and the natural frequencies as shown in Figs. 2 and 3.

· *For the across wind direction*

According to Eq. (4), the change in the frequency is associated with a variation in the critical wind speed \bar{u} . This would lead to a variation in the vortex shedding forces and consequently a variation in the overturning moment acting on the chimney. The tip deflection depends on both the force acting on the chimney as well as the stiffness of the chimney. As both the forces and the stiffness vary similarly with the angle of orientation, no significant change in the tip deflection is expected to occur when the angle θ is altered.

· *For the along wind direction*

The response is mainly static. As such, the external forces are not affected by the change in θ and the corresponding change in the natural frequency. This explains why the along wind peak base overturning moment does not vary with θ . Again, the tip deflection depends on both the external force and the stiffness of the chimney. As the forces do not change and the stiffness varies with θ , a variation of the peak tip deflection is expected to occur when θ is altered.

It could be concluded from the previous discussion that the angle of orientation of the fibers is an excellent design tool for tailoring the laminate to give the optimum structural performance.

4.2. Damping and mass density of FRP

The mass density of FRP materials depends on the percentage of the fibers in the matrix as well as the mass density of both the fibers and the matrix. Since the variation of the mass density of the fibers and the matrix is small, the mass density of FRP composite depends mainly on the percentage of fiber content. The typical density of FRP varies between 1400 kg/m³ for low fiber ratio to 1900 kg/m³ for high fiber ratio.

The across-wind tip deflection (normalized to the diameter) for the previously mentioned chimneys (0.8% damping ratio and $\pm 45^\circ$ angle-ply) are plotted in Fig. 6 versus the mass density of the composite. It should be noted that the mass density has been varied by changing the percentage of the fibers which consequently changes the stiffness of the composite. As seen in Fig. 6, a sharp increase in the tip deflection occurs with the decrease of the mass density. That radical increase in the response occurs when the total damping of the system approaches zero. In view of Eq. (8), a decrease in the mass density of the chimney leads to an increase in value of the negative aerodynamic damping associated with vortex shedding and consequently a decrease in the total damping of the structure. This sharp increase in the response may be shifted to the right or left depending on the damping ratio and the average diameter over the upper third part of the chimney (the region having significant amplitudes of vibration). In general, FRP materials have light weight compared to other structural materials. By examining Eq. (8), it can be stated that due to their light weight, FRP chimneys are expected to experience relatively higher negative aerodynamic damping in the vicinity

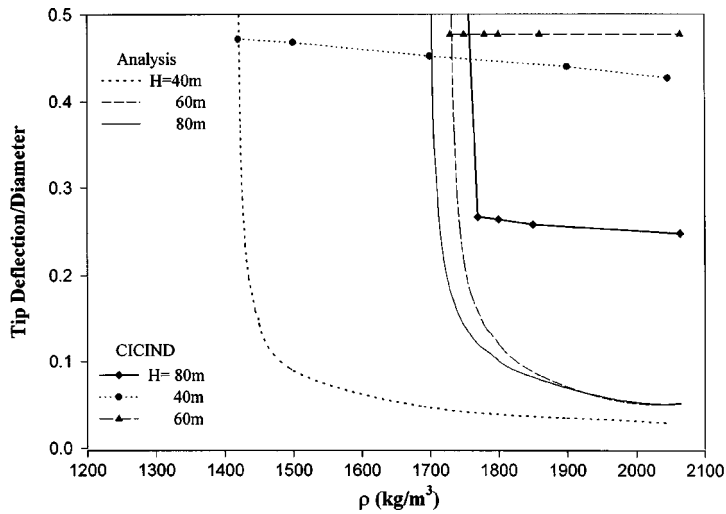


Fig. 6 Normalized across-wind tip deflection versus the mass density

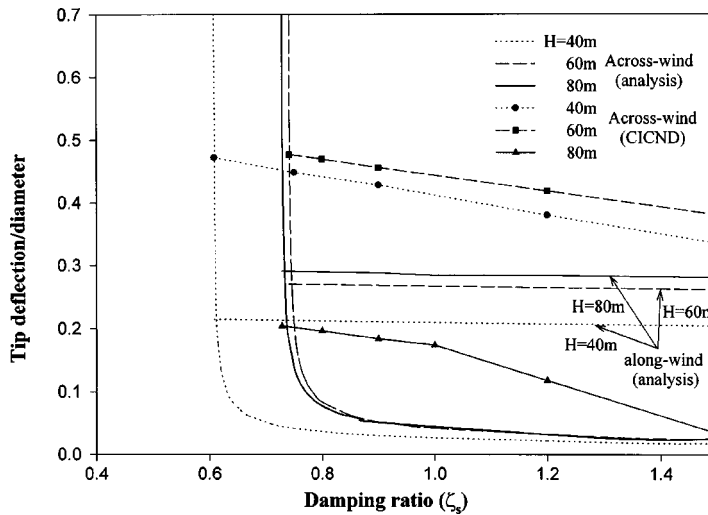


Fig. 7 Normalized tip deflections versus damping ratio

of the critical wind speed compared to steel and concrete chimneys. The negative aerodynamic damping should be compensated by sufficient material damping or external damping devices to prevent excessive oscillations.

The same chimneys are analyzed using variable structural damping ratios with an angle-ply $\theta = \pm 45$ and 70% fibers content. Fig. 7 shows the variation of both along and across-wind response with the damping ratio. It is clear that the along-wind response is not sensitive to the damping ratio. This is due to the fact that the along-wind response is governed mainly by the static components (mean and background) and the resonant component (affected by the damping ratio) has a little effect. On the other hand, the damping ratio has a significant contribution to the across-wind response which represents a resonant response as mentioned before. It is noted that the variation of damping

ratio has the same effect as the variation of the mass density since both of them contribute directly to the total damping of the structure.

The damping of FRP materials depends on a large number of parameters; the fiber orientation, stacking sequence of the layers, amplitude and frequency of vibration and the manufacturing process. As shown in Figs. 6 and 7, the location of the critical response zone varies significantly with the two main parameters which influence the total damping of the structure: structural damping, aerodynamic damping. With the uncertainty about the proper damping ratio for FRP materials, the designer of a FRP chimney should be conservative in estimating the damping ratio in order to ensure the stability of the chimney against vortex shedding. Otherwise, by overestimating the damping ratio, the chimney might become located in the critical region of the across-wind response. In fact, the vortex shedding response is considered the second reason beyond the failure of steel chimneys after chemical corrosion.

In Figs. 6 and 7, the across-wind response are calculated using the CICIND code (1988) for Steel Chimneys and are plotted versus the mass density and the damping ratio, respectively. It is clear from these figures that the CICIND code provides a very conservative response for these three chimneys.

4.3. Effect of tapering

The tapering ratio is another important parameter that influences the across-wind response by varying both the spectrum of the lift forces and the value of the aerodynamic damping. Tapering disperses the frequency of the excitation forces along the height of the chimney. This dispersion makes the spectrum of the lift forces flatter and reduces the dynamic effect of the vortex forces.

To investigate the effect of tapering on the maximum response of FRP chimneys, the across-wind response due to vortex shedding has been calculated for the second chimney (having a height of 60 m) for tapering ratios T equal to 0.0, 0.25 and 0.5, respectively. The tapering ratio T is defined by the following relation : $T = (D_b - D_t)/D_b$; where D_b and D_t are the bottom and the top diameters

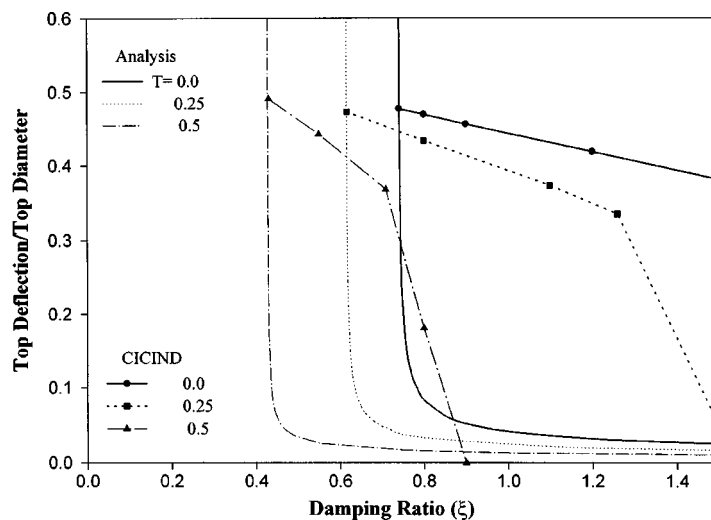


Fig. 8 Across-wind response versus damping ($H = 40$ m, bottom diameter $D_b = 3.75$ m).

of the chimney, respectively. The tapering has been achieved by fixing the bottom diameter $D_b = 3.75$ m and reducing the top diameter D_t . Fig. 8 shows the across wind response plotted versus the damping ratio of the structure ζ_s . As expected, the vortex response is reduced with the increase of the tapering ratio of the chimney. It is noted from Fig. 8 that the region in which the response rapidly increases is shifted to lower damping ratios when chimneys are tapered. As previously discussed, the rapid change in the response occurs when the total damping ratio approaches a zero value. As seen in Fig. 8, providing 0.5 tapering ratio reduces the needed structural damping by about 0.3%. This small percentage is significant when compared to values of the structural damping for steel and FRP materials.

The responses of the same three chimneys, based on the CICIND (1988), are also shown in Fig. 8. It can be seen from the figure that the values predicted by the CICIND are very conservative for all the tapering ratios.

5. Conclusions

This paper starts by describing a computer code that was developed to study the along and across wind responses of FRP chimneys. The code is based on the classical lamination theory, the Stodola method and a procedure for wind loads evaluation that is based on previous studies by Davenport (1993) and Vickery and Basu (1983). The code was verified using a detailed finite element analysis and then used to perform a parametric study for the wind behaviour of FRP chimneys. The parametric study involved investigation for the effect of the angle of fibers orientation, the damping and mass density of the material, and the tapering ratio on the along and across wind responses of FRP chimneys. The study also included an investigation for the adequacy of using the CICIND steel model when attempting the design of a FRP chimney.

From the parametric study conducted in this investigation, one can conclude the following :

- The fiber orientation defines most of the laminate properties such as stiffness, strength and damping ratio. To achieve a considerable improvement in the longitudinal stiffness of the chimney, fibers have to be oriented by an angle $\theta \geq 55^\circ$ (θ is measured with a horizontal direction).
- The tip deflection in the across wind direction is independent of the variation of the angle of fibers orientation θ . On the other hand, the same deflection in the along wind direction depends significantly on the angle of fibers orientation. The maximum values of the along wind tip deflection occur in the vicinity of $\theta = 35^\circ$.
- The overturning moment due to along wind excitation has no variation with the angle of fibers orientation. Meanwhile, the overturning moment resulting from the across wind vibration depends on the value of this angle of orientation; minimum values of this moment occur in the vicinity of $\theta = 35^\circ$.
- The across-wind load response of FRP chimneys is very sensitive to the combined effect of the composite mass density and the damping ratio. Since FRP are very light materials and do not have a well defined damping ratio, a conservative approach must be used in estimating the across-wind response of such chimneys.
- Tapering ratio is a very efficient way of reducing the vortex shedding response.
- The parametric study conducted in this investigation shows that the CICIND code for steel chimneys (1988), when applied to FRP chimneys, leads to conservative estimates for the wind response of the chimneys.

References

- ACI1307-95, American Concrete Institute.
- Berg, G.V. (1989), *Elements of Structural Dynamics*, Prentice Hall, Englewood Cliffs, New Jersey.
- CICIND Model Code for Steel Chimneys, May 1988.
- Davenport, A.G. (1993), "The response of slender structures to wind", *Proceedings of the NATO Advanced study Institute At Waldbronn, wind Climates in Cities*, Germany.
- EUROCOMP (1997), Design Code of FRP.
- Koziey, B.L. (1993), *Formulation and Applications of Consistent Shell and Beam Elements*, Ph.D. Thesis, McMaster University, Hamilton, Canada.
- Koziey, B.L. and Mirza, F.A. (1997), "Consistent thick shell element", *Computers & Structures*, **65**(4), 531-549.
- Jones, R.M (1975), *Mechanics of Composite Materials*, McGraw-Hill Book Company, New York, NY.
- Plecnik, J.M., Whitman, W.E., Baker, T.E. and Pham, M. (1984), "Design concepts for tallest free-standing fiberglass stack", *Polymer Composites*, **5**(3), 186-189.
- Scurton, C. (1963), "On the wind excited oscillations of stacks, towers and masts", *Int. Conference of Wind Effects on Buildings and Structures*, N.P.L. Teddington.
- Van Koten, H. (1969), "Vortex excitation of slender structures", *Proceeding of Conference on Tower-Shaped Structures*, The Hague, Int. Assn. Shell Structures.
- Vickery, B.J. (1997), "Wind loads & design criteria for chimneys", *8th U.S National Conference on Wind Engineering*, Johns Hopkins, Baltimore, Md..
- Vickery, B.J. and Basu, R.I. (1983), "Across-wind vibration of structures of circular cross-section", Part I and II, *J.W.E. and I.A.*, **12**, 49-97.
- Vickery, B.J. and Steckley, A. (1993), "Aerodynamic damping and vortex excitation on an oscillating prism in turbulent shear flow", *J.W.E and I.A.*, **49**, 121-140.

(Communicated by Ahsan Kareem)